Article

Evaluation of Error in IMERG Precipitation Estimates under Different Topographic Conditions and Temporal Scales over Mexico

Yandy G. Mayor, Iryna Tereshchenko *, Mariam Fonseca-Hernández, Diego A. Pantoja and Jorge M. Montes

Department of Physics, University Centre for Exact Sciences and Engineering, University of Guadalajara, Guadalajara 44430, Jalisco, Mexico; yandy.glez.m@gmail.com (Y.G.M.); mariamfnsc@gmail.com (M.F.-H.); diegoseb1@gmail.com (D.A.P.); jorge.montes.a@gmail.com (J.M.M.)
* Correspondence: itereshc@gmail.com; Tel.: +52-333-809-9524

Abstract: This study evaluates the precipitation product of the Integrated Multi-satellitE Retrievals for Global Precipitation Measurement (IMERG) over the Mexican region during the period between April 2014 and October 2015 using three different time scales for cumulative precipitation (hourly, daily and seasonal). Also, the IMERG data have been analyzed as a function of elevation given the rain gauges from the automatic meteorological stations network, located within the area of study, which are used as a reference. In the present study, continuous and categorical statistics are used to evaluate IMERG. It was found that IMERG showed better performance at the daily and seasonal time scale resolutions. While hourly precipitation estimates reached a mean correlation coefficient of 0.35, the daily and seasonal precipitation estimates achieved correlations over 0.51. In addition, the IMERG precipitation product was able to reproduce the diurnal and daily cycles of the average precipitation with a trend towards overestimating rain gauges. However, extreme precipitation events were highly underestimated, as shown by relative biases of −61% and −46% for the hourly and daily precipitation analysis, respectively. It was also found that IMERG tends to improve precipitation detection and to decrease magnitude errors over the higher terrain elevations of Mexico.

Keywords: Integrated Multi-satellitE Retrievals for Global Precipitation Measurement (IMERG); satellite precipitation estimates; statistical analysis; remote sensing; Mexico

1. Introduction

For numerical models verifications, observational data are essential. A network of meteorological observation stations is placed around the world to observe weather and provide data for this purpose; however, this network is still insufficient. Therefore, sounding, radar technology and satellite systems have been added since the past century to overcome the lack of information on all meteorological variables by giving improved spatial (horizontal and vertical) coverage of the meteorological state.

For the particular case of precipitation, the Tropical Rainfall Measuring Mission (TRMM) products gave scientists the opportunity to verify their numerical models simulations from a satellite perspective. However, the satellite responsible for gathering the precipitation information was shut down, and consequently, a new version of these products has been created: the Global Precipitation Measurement (GPM; [1]). The GPM satellite constellation is now generating the new precipitation product called IMERG (Integrated Multi-satellitE Retrievals for GPM). The IMERG product possesses higher temporal and spatial resolutions (30 min and ~11 km) compared with those of TRMM products (3 h and ~25 km).

The availability of this precipitation product brought the opportunity for these models verification at higher resolutions. However, the main problem with all new satellite precipitation products is the lack of evaluation and that they are not thoroughly tested for all regions. For example, Wang et al. [2] briefly analyzed the IMERG product and found an overall agreement with the previous TRMM data set. Huffman et al. [1] mentioned that monthly and daily precipitation gauges were used to improve, at least in some regions, the biases that characterize the IMERG precipitation estimates. However, concerns regarding the quality of this data set at higher temporal resolutions still remain due to the relative novelty of the IMERG precipitation product. Other studies have been made worldwide that help improve our understanding of the IMERG precipitation product [3–6]. Sharifi et al. [3] assessed the GPM–IMERG final run against gauge data over four small regions in Iran, with diverse topography and climate conditions. They also compared IMERG with the ERA-Interim product from the European Centre for Medium Range Weather Forecasts (ECMWF) and TRMM data and found that IMERG performed better for heavy, daily precipitation. Ma et al. [4] also compared IMERG with TRMM and gauge data at a three-hourly scale over the Tibetan Plateau and found that IMERG performed better for light and solid precipitation at higher elevations than TRMM. Rios Gaona et al. [5] compared IMERG against gauge-adjusted radar rainfall data at different time scales over the relatively flat terrains of the Netherlands. An overall underestimation of the IMERG data and higher correlations with increasing time scales were found. Also, Guo et al. [7] provided a quantitative study of error characteristics of the IMERG over China. Here, it was found that this satellite product overestimates light rainfall events over arid areas. All this research focused its analysis on particular areas of interest. However, there is no study, to our current knowledge, that evaluates the IMERG precipitation dataset over the Mexican region.

Mexico is a developing country which relies on a sparse rain-gauge network to provide the rainfall data needed to manage their water resources. Although these water resources are not scarce, they are not equally distributed throughout the region. In addition, Mexico figures as one of the twelve countries with the greatest biodiversity worldwide [8]. Therefore, the estimation and proper management of water resources is of great importance to the country. Also, in remote areas, such as mountains, deserts and oceans, where rain gauges are unable to be installed and radar systems are not available; the satellite-derived rainfall may be the only tool to provide precipitation information with relatively high spatial and temporal resolutions [3].

Therefore, the present study aims to evaluate the IMERG precipitation dataset over the Mexico region by analyzing different time scales of precipitation, such as hourly, daily and seasonal cumulative precipitation. The automatic meteorological network located within this region has been used as the reference since it provides rain gauges at time scales smaller than the analysis scales. This investigation, which is to our knowledge, the first to evaluate the IMERG precipitation data over Mexico, will contribute to a better understanding of the IMERG dataset and it will also open the doors to future studies with hydrological applications over the region.

This article is organized as follows: Section 2 will describe the data, methods and the area of study. In Section 3 results will be presented through three sub-sections that analyze the IMERG data with different time scales of the precipitation. To complement the evaluation study, IMERG is analyzed as a function of the elevation given the location of the automatic meteorological stations. The discussion and conclusions are presented in Sections 4 and 5 respectively.

2. Materials and Methods

In this section, the area of study, the data (IMERG and rain gauges) as well as the statistical measures and methodology used, are described.

2.1. Study Region

The area of study is shown in Figure 1. This area is about 1,154,726.56 km^2 in size, covering almost all of central and northern Mexico. Country boundaries are mostly off the study region; hence they are not shown in Figure 1b. This region presents a wide variety of climates [9], not only determined

by the mean atmospheric conditions but also due to the heterogeneity of the orography. The main mountainous systems of the country, such as the Sierra Madre Occidental, the Sierra Madre Oriental as well as the Mexican Altiplano systems are represented in the area of study. Also, the automatic meteorological stations used in this research are representative of the wide range of elevations and climates throughout the area shown in Figure 1b.

The area of study is located between 17.1 and 27.7 degrees north (17°6′0″N–27°42′0″N) and 96.4 and 113.6 degrees west (96°24′0″W–113°36′0″W). It is worth noting how variable and complex the topography is in the area, where elevations can be higher than 4000 m.

The regimen of precipitation varies greatly from north to south. The northern areas in Figure 1b receive precipitation below 500 mm per year and there are increases towards the south up to annual precipitations over 3000 mm. Precipitation also varies from the coast to inland in the continental region (coastal regions receive more precipitation) while the Peninsula of California is mostly dry with annual precipitations below 500 mm. The majority of the annual precipitation in the territory falls from June to September during the rainy season, when the continental anticyclone weakens and convergence of warm, moist air prevails over the central and southern region. The precipitation on the northwest of the main land also occurs during the rainy season and is related to the North American monsoon [10,11].
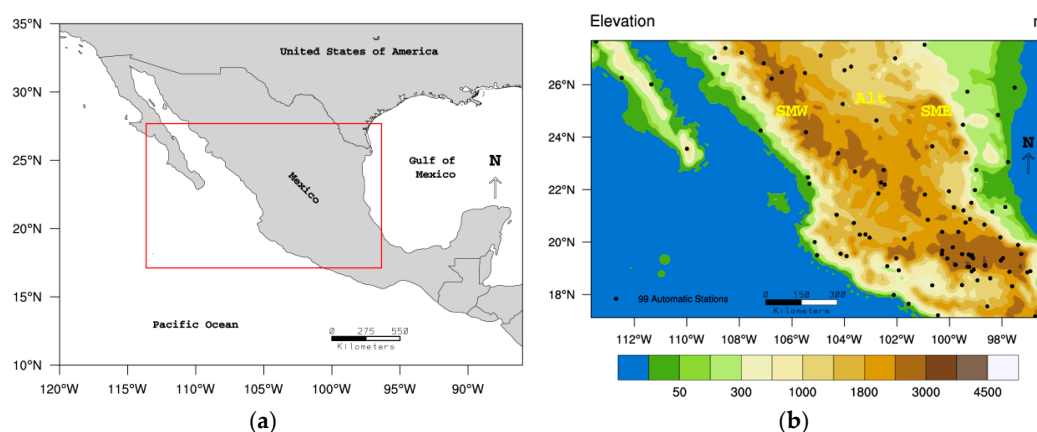

Figure 1. The area of study is enclosed in the red polygon (**a**) and automatic meteorological stations shown in black dots (**b**). Note the irregularity shown in the topography (color in m). In yellow *SMW* shows the location of the Sierra Madre Occidental, *SME* stands for Sierra Madre Oriental and *Alt* is the Mexican Altiplano.

2.2. IMERG Data

The Integrated Multi-satellitE Retrievals for GPM (IMERG) product was created by intercalibrating, merging and interpolating all satellite microwave precipitation estimates, together with microwave-calibrated infrared (IR) satellite estimates, precipitation gauge analyses, and potentially other precipitation estimators at finer scales from the TRMM and GPM eras over the entire globe. The IMERG data are produced by a Bayesian inverse algorithm applied to microwave brightness temperatures that is run several times for each observation time. IMERG can range from giving a quick precipitation estimate to research-level products as more data are used in the algorithm, including monthly gauges [12].

The GPM core satellite can be considered an improved version of the TRMM satellite. It serves as both a calibration and an evaluation tool for all the passive microwave and infrared-based precipitation products integrated in IMERG. It has wider spatial coverage than TRMM, is sensitive to light precipitation, and it can also differentiate liquid and solid precipitation phases in terms of a probability for the presence of the liquid phase [13].

This study used final half-hourly cumulative precipitation files at a resolution of 0.1 degree of latitude/longitude. Within these files, two variables were created: the multi-satellite precipitation

estimate, with gauge calibration in mm/h (millimeters per hour), and the probability of the liquid precipitation phase; the latter is not used in this research. Half-hourly IMERG version 3 files are available for the period from March 2014 until the present with a few months of lag time (https://storm.pps.eosdis.nasa.gov/storm/). Since the March 2014 runs were suggested to be ignored by Huffman et al. [1], the study period was chosen to extend from 1 April 2014 to 31 October 2015.

The precipitation estimates for precipitation data (P_n, P_{n+1}) in two half-hour periods have been converted into hourly precipitation estimates (P_{hour}) following the mathematical relationship: $P_{hour}(mm) = \left[P_n\left(\frac{mm}{h}\right) + P_{n+1}\left(\frac{mm}{h}\right) \right] * 0.5(h)$. Daily and seasonal precipitation estimates were then created to be used in this research.

2.3. Rain Gauge Data

The rain gauges were obtained from the *CONAGUA* (in Spanish: *Comisión Nacional del Agua*) database (http://smn.cna.gob.mx/es/). These data come from automatic meteorological stations located throughout Mexico. In total, 99 meteorological stations (with a density of one station per 11,663.9 km^2) located within the area of study have been used (Figure 1b) and the entire gauge data were subjected to a quality control procedure. This meteorological network, although insufficient, is at this moment the best source of high-resolution precipitation data for our area. It gathers cumulative precipitation in mm every 10 min. In this case, hourly, daily and seasonal cumulative precipitation has been used instead.

2.4. Evaluation Procedures

In order to compare observed precipitations with IMERG estimates, some interpolation needs to be done. To avoid the modification of the actual observation data, an alternative grid to point interpolation technique is used in this study. The procedure consists of using a bilinear interpolation method on the IMERG estimates data to obtain the precipitation at the specific points corresponding to the meteorological stations where the precipitation data were collected. Hereafter, these points will be referred to simply as meteorological stations. The bilinear interpolation method uses the distance-weighted average of the four nearest grid nodes values to give an estimate at a point of interest. This method also assumes high correlations between data points, which can be expected in this case, due to the relatively high resolution of the satellite precipitation product. Accadia et al. [14] showed that the application of the bilinear interpolation to precipitation fields with spatial resolution of about 10 km may introduce bias since it does not conserve total precipitation and results in smoothing of the precipitation field by increasing the minima and reducing the maxima. However, this interpolation method has been satisfactorily used in previous studies [15,16].

Statistical measures can be divided into different categories. In this study, continuous and categorical statistics are used to characterize IMERG from hourly, daily and seasonal precipitation estimates.

2.4.1. Continuous Evaluation Statistics

The continuous statistical measures used in this study are the Pearson correlation coefficient (*COR*), the bias (*BIAS*), the relative bias (*RBIAS*) and the root-mean-square error (*RMSE*) shown in Equations (1)–(4) respectively. These measures have been utilized before in evaluation studies of precipitation [3,17,18] and are described in detail in Ebert et al. [19].

The *COR* ranges from −1 to 1. Zero values mean there is no correlation between the estimated and observed fields, while non-zero values indicate a linear relationship between the fields. In the case of the *BIAS*, zero is the desirable value, which means there is no bias between estimated and observed fields, whereas positive (negative) values indicate that the estimated field overestimates (underestimates) the observations. The *RBIAS* describes the systematic bias of satellite precipitation and behaves the same as bias. Meanwhile, the *RMSE* function emphasizes extremes and does not give the direction of the deviations.

$$COR = \frac{\sum_{i=1}^{N}(E_i - \overline{E}) * (O_i - \overline{O})}{\sqrt{\sum_{i=1}^{N}(E_i - \overline{E})^2} * \sqrt{\sum_{i=1}^{N}(O_i - \overline{O})^2}} \tag{1}$$

$$BIAS = \frac{1}{N}\sum_{i=1}^{N}(E_i - O_i) \tag{2}$$

$$RBIAS = \frac{\sum_{i=1}^{N}(E_i - O_i)}{\sum_{i=1}^{N}O_i} * 100 \tag{3}$$

$$RMSE = \sqrt{\frac{1}{N}\sum_{i=1}^{N}(E_i - O_i)^2} \tag{4}$$

In the equations, *E* stands for the Estimated or modeled values, and *O* stands for Observations. *N* is the length of the estimated and observed fields. The variables with bars on top denote the mean values of the corresponding field.

2.4.2. Categorical Evaluation Statistics

The categorical statistics used in this study are the false alarm ratio (*FAR*), the probability of detection (*POD*), the critical success index (*CSI*) and the accuracy (*ACC*) shown in Equations (5)–(8). These measures have also been widely used [3,5,20] and are described in detail in Wilks [21].

The *FAR* lies between 0 and 1, where 0 is the desired result. The *POD* and *CSI* also range from 0 to 1. For these two statistics 1 is the perfect score. Both metrics tell the accuracy with which the satellite correctly estimates the rainfall events but the *CSI* also considers the false alarms. Finally, the *ACC* measures the fraction of correct satellite estimates and its perfect score is 1.

$$FAR = \frac{b}{a+b} \tag{5}$$

$$POD = \frac{a}{a+c} \tag{6}$$

$$CSI = \frac{a}{a+b+c} \tag{7}$$

$$ACC = \frac{a+d}{a+b+c+d} \tag{8}$$

where *a, b, c, d* are the possible events shown in Table 1.

Table 1. Contingency table of possible events.

		Observed Precipitation	
		Yes	**No**
Estimated precipitation	**Yes**	Hits (*a*)	False alarms (*b*)
	No	Misses (*c*)	Correct rejections (*d*)

Finally, a threshold of 0.1 mm has been used to differentiate precipitation and no precipitation events since precipitation values below this threshold may be the result of noise. Although the selection of this threshold is subjective, Tan et al. [22] found that their results remained robust when they repeated the analysis for higher thresholds.

3. Results

In this section results are presented using continuous and categorical statistics with hourly, daily and seasonal cumulative precipitation. It is believed that using different temporal resolutions would lead to

more comprehensive details of the characteristics of the IMERG precipitation product. Also included is an elevation analysis using both continuous and categorical statistics. This will help understand the IMERG data behavior in capturing precipitation and its intensity depending on topography.

3.1. Hourly Analysis

Figure 2 describes the variation of the mean hourly rainfall for the studied period and for all meteorological stations where gauge and IMERG data were computed. Highest values of the mean hourly rainfall are found during the late afternoon and night-time hours. The lowest values correspond to hours between 07:00 and 20:00 UTC hours, reaching a minimum between 15:00 to 17:00 UTC hours. Additionally, a lag of approximately 2 h between the hourly minimum and maximum peaks of the IMERG and the rain gauge data is observed. Moreover, where higher values are found, IMERG seems to overestimate gauge data, while it underestimates gauge data for lower mean hourly precipitations. Overall, it can be seen that the IMERG data reproduce the daily cycle of the average precipitation over the study area fairly well, although it appears that the IMERG product behaves differently (with respect to gauges) during daytime and night-time hours.

Also, hourly correlation (blue), bias (yellow) and root-mean-square error (green) average values are presented in Figure 2. Mean statistics were computed for each hour and for all meteorological stations. In Figure 2, it is shown that hourly correlations range from 0.25 to 0.5. Biases are close to 0 mm/h with a slight trend for IMERG to overestimate gauge data during night-time hours. As shown in Figure 2 the *RMSE* values range from 0.2 to 1.5 mm/h and follow IMERG hourly trends. Note that minimum values for *RMSE* are found during daytime hours when correlations are higher.
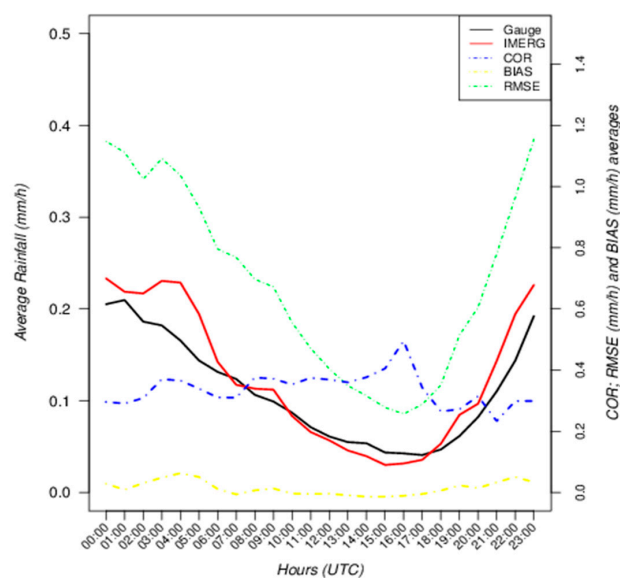

Figure 2. Average hourly rainfall (mm/h) for Integrated Multi-satellitE Retrievals for Global Precipitation Measurement (IMERG) (red) and Gauge (black) data for the period 1 April 2014 to 31 October 2015. Hourly average statistics results are shown. Pearson correlation coefficient (*COR*): blue; bias (*BIAS*) (mm/h): yellow; and root-mean-square error (*RMSE*) (mm/h): green, for the same period.

IMERG's ability to capture extreme rainfall events has been also analyzed in this study. For this, the 98th to 99.99th percentile of the observed precipitation values have been compared with their corresponding IMERG estimates. Table 2 shows the statistics resulting from this comparison. Here, a bias of -2.7 mm/h indicates that IMERG tends to underestimate extreme precipitations. The *RBIAS* shows that IMERG precipitation estimates account for only 61% of the mean rain gauges for precipitation intensities between 1.2 and 35.79 mm/h. In addition, the *RMSE* indicates that mean deviations are higher than 5 mm/h, which is considered large because it is four times higher than the

minimum (1.2 mm/h) and also because of the weak correlation value of 0.18. We also analyzed the behavior of the very extreme rainfall events (cases above the 99.99th percentile) with similar results (See Figure S1 and Table S1). Here the underestimation of IMERG increased remarkably to 89%.

Table 2. Extreme events statistics. Hourly analysis.

Number of Events	Min (mm/h)	Max (mm/h)	COR	BIAS (mm/h)	RMSE (mm/h)	RBIAS (%)
27,670	1.20	35.79	0.18	−2.70	5.82	−61.00

Also in this section, continuous and categorical statistics are used to describe the IMERG characteristics with respect to gauge locations. This analysis gives a spatial perspective of the IMERG behavior. To this end, Figure 3 shows correlations statistics. Figure 3a shows correlations as a function of the location of the meteorological stations, colors are given by correlation intervals; Figure 3b is a scatter plot diagram for gauge vs. IMERG hourly precipitations for all meteorological stations and Figure 3c shows the actual correlations values (red line) for each meteorological station, which have been ordered following their elevations (gray, shaded area). The regression line (in black) shown in Figure 3c describes the relationship between the correlation and topography.
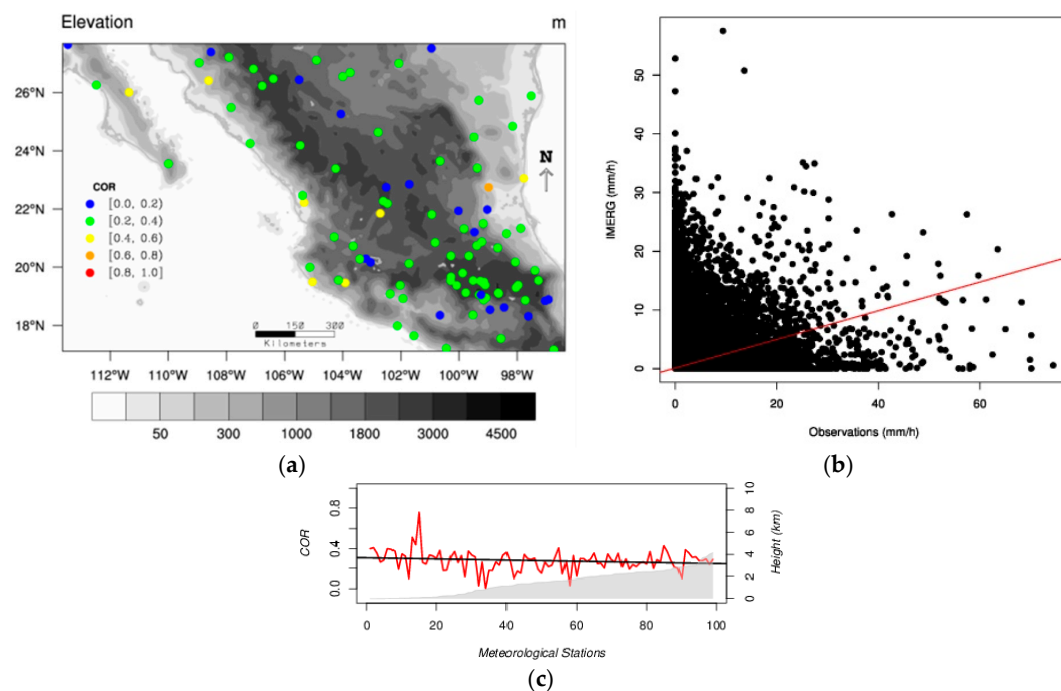

Figure 3. (**a**) Correlation (*COR*) map; (**b**) scatter plot for hourly precipitation events and (**c**) correlation as a function of meteorological stations elevations (red line); the black line shows the trend and the elevation of the meteorological stations is represented by the gray, shaded area. IMERG estimates and gauge hourly data from 1 April 2014 to 31 October 2015 have been used for these calculations.

It can be noted from Figure 3a that most meteorological stations show correlation values between 0.2 and 0.4. However, a slight trend is observed for some meteorological stations located at higher elevations to have correlation values below 0.2, while some others closer to the coast and located at lower elevations show correlation values higher than 0.4. Figure 3c confirms this slight trend.

The scatter plot in Figure 3b confirms one of the main characteristics of the precipitation: its mode is not to precipitate. The shape of the scatter plot suggests that the probability for IMERG to overestimate the observed precipitation increases for precipitation intensities below 5 mm/h. On the contrary, IMERG

most likely underestimates rain gauges for precipitation intensities above this value. Above 5 mm/h, the probability of underestimation by IMERG increases with increasing observed rainfall intensities.

Figure 4a,c for the *RBIAS* and Figure 4b,d for the *RMSE* are homologous to Figure 3a,c respectively. Figure 4a shows that for more than the half of the meteorological stations IMERG overestimates hourly rain gauges. Also, it can be noticed that overestimations values are higher than the underestimation values. For some meteorological stations the overestimation can be two or three times higher than their mean hourly rain gauges. In addition, Figure 4c shows that the relative bias clearly decreases with elevation.

Figure 4b shows that the *RMSE* values are below 2.5 mm/h. However, the majority of the stations show *RMSE* values between 0.5 and 1.0 mm/h. In Figure 4d, the trend for *RMSE* with respect to topography is flatter than that for *RBIAS* (Figure 4c) and only a very slight trend of the *RMSE* values to decrease as the elevation increases can be observed.

Categorical statistics (*FAR*, *POD*, *CSI* and *ACC*) for hourly precipitation data are shown in Figure 5 in the same manner that the *RBIAS* and *RMSE* have been shown in Figure 3. Therefore, each categorical statistic is represented in a map to analyze spatial behavior and in a trend plot to analyze its relationship with respect to the elevation of the meteorological stations.

For hourly precipitation data it can be noticed that the *FAR* values (Figure 5a) are higher than the *POD* values (Figure 5b) for all meteorological stations. Note that accurate IMERG estimates imply that the *FAR* values are close to 0 while the *POD* values are close to 1. However, values for the *FAR* are greater than 0.4 and values between 0.6 and 0.8 are more common. Meanwhile, values for the *POD* are below 0.8 and the most common values range from 0.4 to 0.6. The *FAR* in Figure 5c shows more sensitivity to elevation than the *POD* and the general trend of these values is to decrease with increasing elevations.
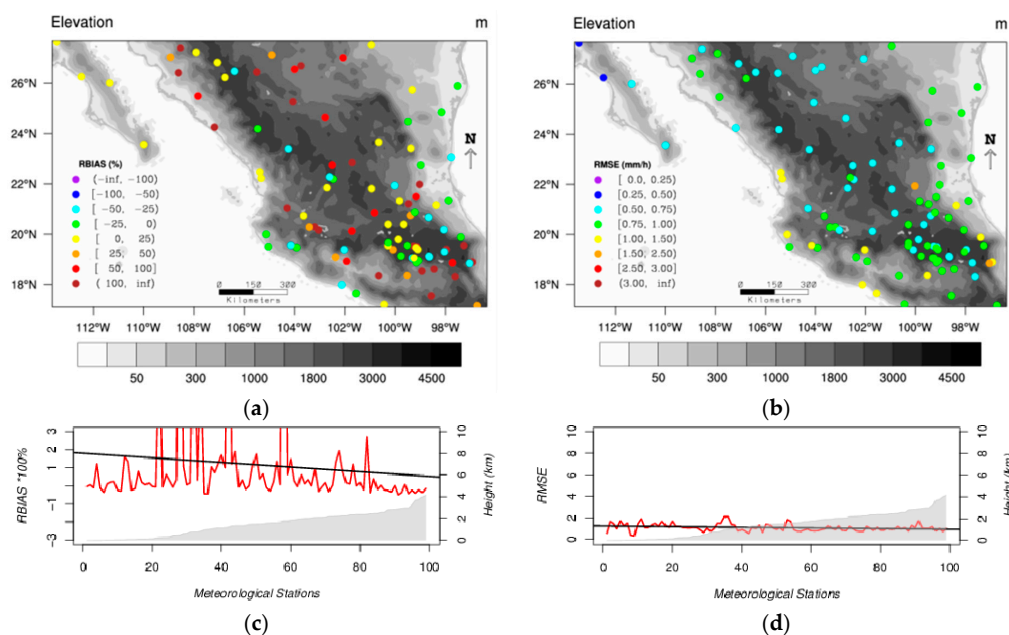

Figure 4. (**a**) Relative bias (*RBIAS*) map; (**b**) root-mean-square error (*RMSE*) map; (**c**) and (**d**) are the *RBIAS* and *RMSE*, respectively, shown as a function of meteorological stations elevations (red lines); the black lines show the trends and the elevation of the meteorological stations is represented by the gray, shaded area. IMERG estimates and gauge hourly data from 1 April 2014 to 31 October 2015 have been used for these calculations.
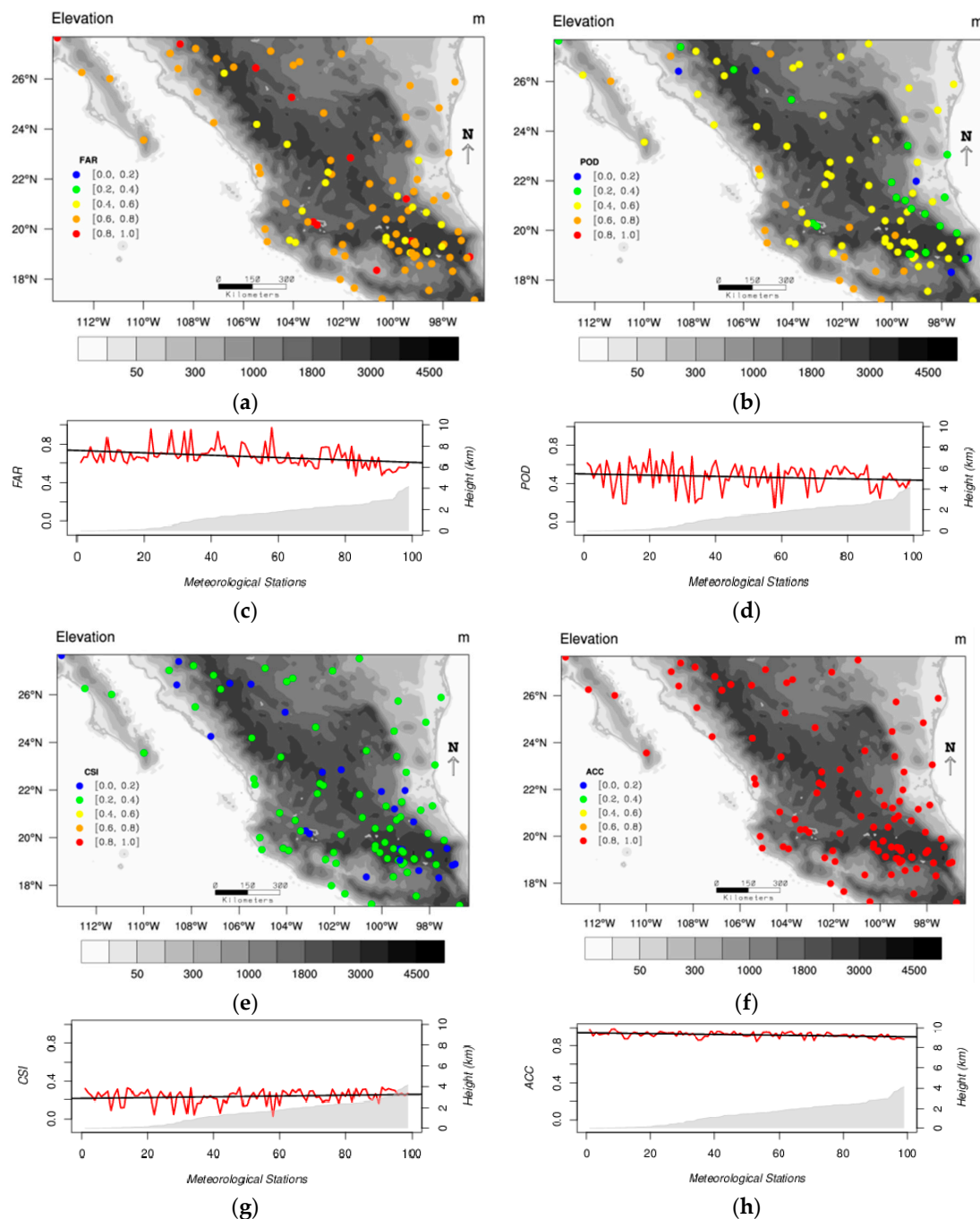
Figure 5. (**a**) False alarm ratio (*FAR*) map; (**b**) probability of detection (*POD*) map; (**e**) critical success index (*CSI*); (**f**) accuracy (*ACC*) map; and (**c**), (**d**), (**g**) and (**h**) are the *FAR*, *POD*, *CSI* and *ACC*, respectively shown as a function of meteorological stations elevations (red lines); the black lines show the trends and the elevation of the meteorological stations is represented by the gray, shaded area. IMERG estimates and gauge hourly data from 1 April 2014 to 31 October 2015 have been used for these calculations.

Figure 5e,f also show two categorical measures that characterize the degree of accuracy by which IMERG represent hourly rain gauges. However, both measures seem to differ in how accurate IMERG is. *CSI* values in Figure 5e range between 0 and 0.4 and a slight trend to increase with elevation can be observed in Figure 5g. However, *ACC* values are very high, ranging between 0.8 and 1.0 (see Figure 5f) and its trend in Figure 5h is shown to decrease with increasing elevations.

3.2. Daily Analysis

In Figure 6 the average daily rainfall for the whole study period is presented. Average values were calculated using all meteorological stations. The thick red and black lines resulted from smoothing raw IMERG and gauge average daily rainfall respectively so that trends can be easily analyzed. The smoothing procedure consists of applying locally weighted regression to scattered data [23]. In this figure, the dry and wet seasons during the study period can be easily noted. During the dry season (November to April [9]) average daily rainfall falls under 1 mm (see trend lines) and reaches higher values during the wet season. It is also shown that IMERG better represents the daily precipitation in the dry season and during the wet season IMERG mostly overestimates gauge data. Moreover, average daily rainfall values can reach over 18 mm/day during extreme precipitation events.

In addition, Figure 6 shows the *COR, BIAS* and *RMSE* values calculated with IMERG and gauge daily rainfall data. A *COR* value of 0.54 shows that daily IMERG estimates improve its agreement with respect to the hourly analysis. The bias indicates an overall overestimation of IMERG of 0.34 mm/day. Meanwhile an *RMSE* value of 7.93 mm/day indicates that the deviations can be significant considering an average daily rainfall below 4 mm/day.

Daily precipitation extremes have been also analyzed. Extreme rainfall events were determined by choosing the 98th to 99.99th percentile of the daily precipitation distribution from gauge data. Table 3 shows the statistics calculated for these data as compared with their corresponding IMERG 24-h precipitation estimates.
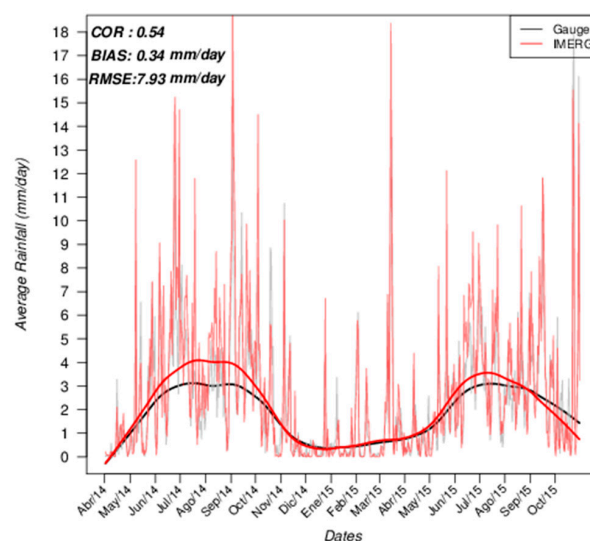

Figure 6. Average daily rainfall (mm/day) for IMERG (thin pink) and gauge (thin gray) data from 1 April 2014 to 31 October 2015. Thick red and black lines resulted from smoothing raw IMERG and gauge data respectively. The *COR, BIAS* and *RMSE* values shown in the figure were calculated for these data.

Table 3. Extreme events statistics. Daily analysis.

Number. of Events	Min (mm/day)	Max (mm/day)	COR	BIAS (mm/day)	RMSE (mm/day)	RBIAS (%)
1141	26.92	180.59	0.36	−21.03	34.55	−46.00

The *BIAS* and *RBIAS* in Table 3 indicate that IMERG keeps underestimating rain gauges for extreme precipitation events. IMERG underestimates 46% of daily rain gauges, which is significantly less than that for the hourly analysis. The minimum daily precipitation considered here is about 27 mm/day; hence a deviation of 34.55 (see *RMSE*) shows also an improvement relative to the hourly analysis. The correlation (0.36) is also better than for the hourly analysis. Therefore, it can be said that IMERG accuracy improves with time scale from hourly to daily extreme precipitation events.

In addition, Figure 7 shows the absolute errors of the mean daily rainfall for each meteorological station and for precipitation intensities of 0–10 mm/day (solid cyan line), 10–25 mm/day (solid blue line) and 25 mm/day or greater (solid green line). These absolute errors were calculated using the mean values of the daily precipitation data (IMERG and gauge) for each station. They represent how much IMERG deviates from the gauge data. For example, the figure shows that for station 1 (x-axis) IMERG deviates from the gauge data in almost 5 mm/day for precipitation intensities of 25 mm/day or greater. Also, the absence of data in green and blue lines means that precipitation intensities corresponding to their respective ranges were not found for the corresponding meteorological station.

What is worth noting in Figure 7 is that there is almost no deviation of IMERG from the precipitation observed when precipitation intensities are less than 10 mm/day. However, when precipitations are higher, the deviation can be over 15 mm/day. Also, there is no appreciable relation between this deviation and the elevation where a meteorological station is located.
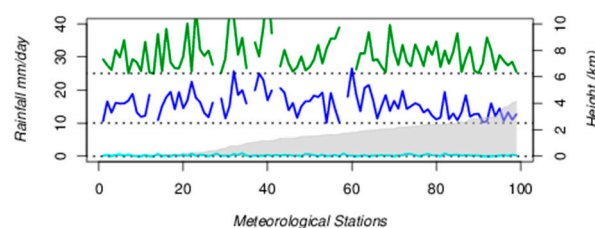

Figure 7. Absolute errors as a function of meteorological stations elevation. Absolute errors were calculated using the IMERG and gauge daily data from 1 April 2014 to 31 October 2015. Lines show the absolute errors for precipitation intensities ranging between 0 and 10 mm/day (cyan), 10 and 25 mm/day (blue) and over 25 mm/day (green).

Also in this section, continuous and categorical statistics are used to describe the IMERG characteristics with respect to gauge locations. This analysis gives a spatial perspective of the IMERG behavior for the daily analysis. To this end, Figure 8 shows correlations statistics in the same way it was presented in Figure 3 for the hourly analysis.

In Figure 8a correlations are good for most meteorological stations. *COR* values between 0.4 and 1.0 dominate, while only a few stations show correlations below 0.4. A flat regression line in Figure 8c indicates no relation between *COR* and the elevation of the meteorological station.

The scatter plot in Figure 8b shows that daily precipitation intensities below 75 mm/day are the most common. The shape of the plot also suggests that IMERG tends to overestimate rain gauges for small precipitation amounts and underestimates them for large rainfall. It is not clear here what threshold to select, for IMERG switches from underestimating to overestimate daily rain gauges but it should be between 10 and 50 mm/day.

In a manner similar to that of Figure 4, Figure 9 shows the *RBIAS* and *RMSE* statistics for the daily analysis. Figure 9a shows that the bulk of the stations have *RBIAS* ranging between −50 and 50%; while most of the rest of the stations significantly overestimate observations. The trend of the *RBIAS* in Figure 9c indicates that the overestimation decreases with elevation.

RMSE values in Figure 9b are found to increase toward south of the region where more precipitation occurs. Also, *RMSE* tends to decrease from the coast toward inlands. These trends seem to be dominant over any relationship that may exist between the *RMSE* and the elevations of the meteorological stations. Note that Figure 9d shows only a slight trend for *RMSE* to decrease with terrain elevation.

Categorical statistics (*FAR, POD, CSI* and *ACC*) for daily precipitation data are shown in Figure 10 in the same manner *RBIAS* and *RMSE* were shown in Figure 9. Therefore, each categorical statistic is represented in a map to analyze spatial behavior and in a trend plot to analyze its relationship with respect to the elevation of the meteorological stations.

Figure 10a,b show that *FAR* values are generally smaller than *POD* values which means that daily IMERG precipitation data are more accurate than the hourly data. *FAR* values are usually smaller than

0.6 while most *POD* values overreach this threshold. Also, *FAR* tends to decrease while *POD* increases with increasing terrain elevations; see Figure 10c,d. These results are consistent with the fact that *CSI* in Figure 10g also increases with elevation. Figure 10e shows most meteorological stations having a *CSI* between 0.4 and 0.8 which represents an improvement over the hourly analysis.
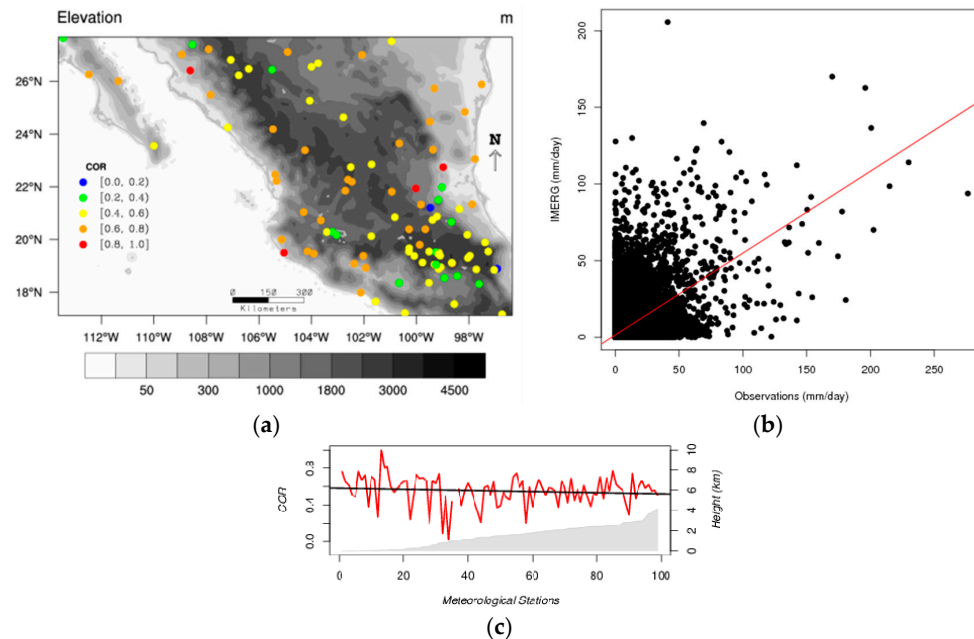

Figure 8. (**a**) Correlation (*COR*) map; (**b**) scatter plot for daily precipitation events and (**c**) correlation as a function of meteorological stations elevations (red line); the black line shows the trend and the elevation of the meteorological stations is represented by the gray, shaded area. IMERG estimates and gauge daily data from 1 April 2014 to 31 October 2015 have been used for these calculations.
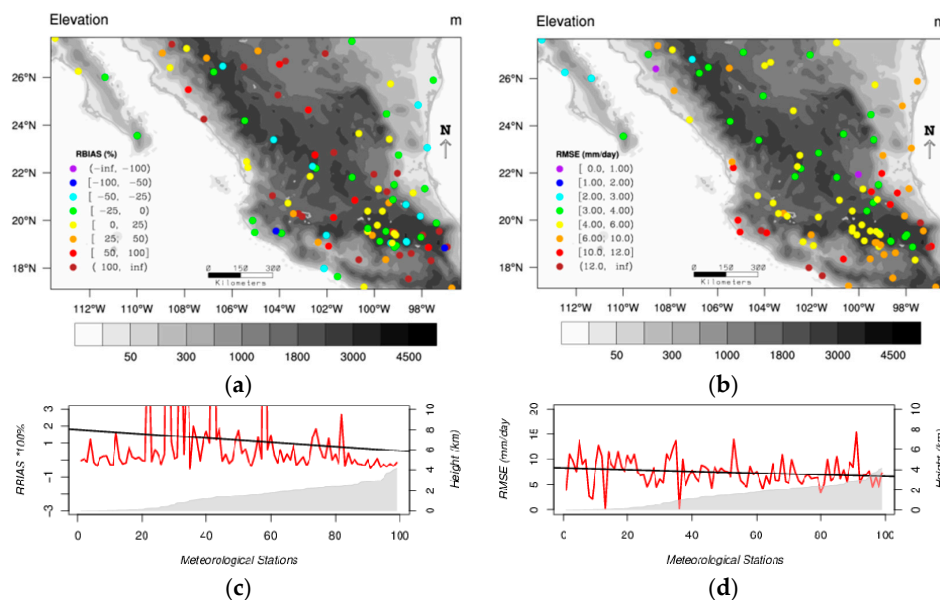

Figure 9. (**a**) Relative bias (*RBIAS*) map; (**b**) Root mean squared error (*RMSE*) map; (**c**) and (**d**) are *RBIAS* and *RMSE*, respectively, shown as a function of meteorological stations elevations (red lines); the black lines show the trends and the elevation of the meteorological stations is represented by the gray, shaded area. IMERG estimates and gauge daily data from 1 April 2014 to 31 October 2015 have been used for these calculations.

The *ACC* in Figure 10f also indicates high accuracy of the IMERG daily precipitation data. However, values are generally smaller than those for the hourly analysis. Figure 10h indicates no relation between the *ACC* and the topography.
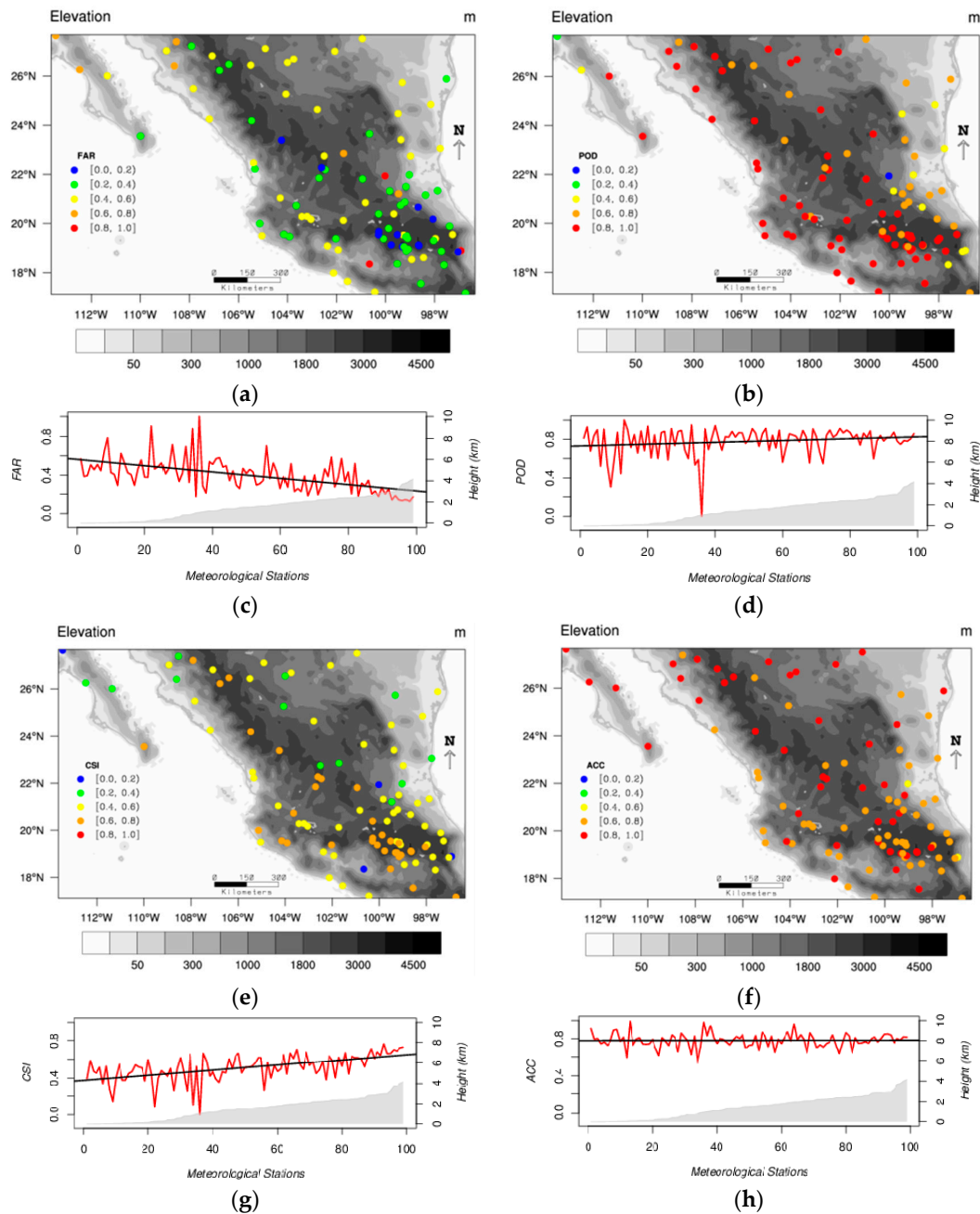

Figure 10. (**a**) False alarm ratio (*FAR*) map; (**b**) probability of detection (*POD*) map; (**e**) critical success index (*CSI*) map; (**f**) accuracy (*ACC*) map; and (**c**), (**d**), (**g**) and (**h**) are *FAR*, *POD*, *CSI* and *ACC*, respectively shown as a function of meteorological stations elevations (red lines); the black lines show the trends and the elevation of the meteorological stations is represented by the gray, shaded area. IMERG estimates and gauge daily data from 1 April 2014 to 31 October 2015 have been used for these calculations.

3.3. Seasonal Analysis

Figure 11 shows the average seasonal precipitation (mm) for the dry and wet seasons and for IMERG and gauge data. The average is calculated using all meteorological stations and the dry season

is considered to be from November to April. Here, it can be noted that during the dry season the average precipitation is close to 200 mm and during wet season that amount is tripled. During the dry season IMERG quantifies the average precipitation quite well and overestimates the precipitation observed during the wet season by approximately 100 mm.

Table 4 shows continuous statistics results for the seasonal precipitation as registered (or estimated) at the meteorological stations using gauge (or IMERG) data. Results here confirm that the IMERG represents the overall precipitation for the dry season better than for the wet season. For instance, the correlation is close to 0.7 for the dry season and close to 0.5 for the wet season. The bias is significantly better for the dry season (approximately 1 mm) than for the wet season (approximately 96 mm). For the *RMSE*, results are not favorable, yet the dry season is still favored.
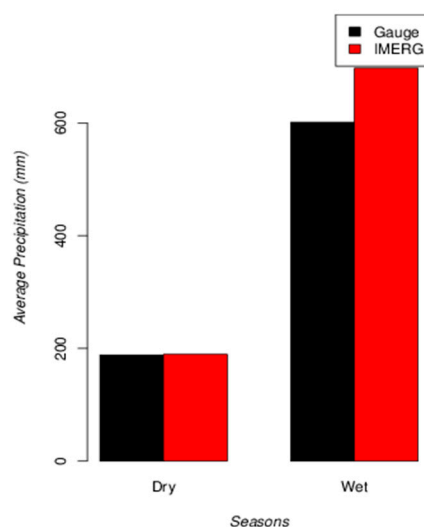

Figure 11. Average seasonal precipitation (mm) for the dry and wet seasons and for IMERG (red bars) and gauge (black bars) data for the period from 1 April 2014 to 31 October 2015. The average is calculated for all meteorological stations and the dry season is considered to be from November to April.

Table 4. Seasonal statistics results. Statistics were calculated for all meteorological stations using IMERG and gauge data from 1 April 2014 to 31 October 2015.

Seasons\Statistics	*COR*	*BIAS* (mm)	*RMSE* (mm)
Dry	0.69	1.11	123.95
Wet	0.51	96.39	355.10

4. Discussion

From results found in this research, it can be said that the IMERG generally captures the trends of the average precipitation observed for all time scales analyzed (hourly, daily and seasonal). However, for the daily precipitation cycle, a 2-h lag in terms of the peak time was observed. Tang et al. [24] found a similar result but with a more severe lag between 2 and 5 h for six sub-regions of China. These lags have been associated to the use of geo-infrared satellites in the estimation of the precipitation [25].

Hourly correlation values of approximately 0.35 (see Figure 2) have been reported previously [4]. It can also be expected that these values get higher as the temporal scale increases [6]. Therefore, correlation results found for the daily (Figure 6) and seasonal (Table 4) analysis are in agreement with the later.

Statistical biases suggest that IMERG tends to overestimate average gauge data for small amounts of precipitation. The study of biases in the satellite-based precipitation products is challenging. Among the many studies that have been conducted, the results vary depending on the study region and the precipitation time scale. For example, Sharifi et al. [3] found that IMERG generally underestimated

rain gauges, but their analysis only included cases with observed precipitation. Ma et al. [4] found overall positive biases over the Tibetan Plateau region using a three-hourly time scale. In addition, it was also observed that the probability for the IMERG to overestimate gauge data decreases with the meteorological station altitude for the hourly and daily precipitation data. Bharti and Singh [20] found that the TRMM precipitation product overestimated rainfall on elevation ranges less than 3000 m but severely underestimated precipitation over higher elevations in the Himalayan region. The relation existing between all satellite precipitation products and the orography is undeniable [4,20,26]. However, in this study this relationship becomes more evident for the daily than for the hourly precipitation.

The differences in biases between regions might be due to the randomly selected number of gauges used for bias correction in satellite products and/or due to the spatial resolution of the satellite-based precipitation estimates [3]. Another source for error in precipitation biases among regions is the types of typical clouds that differ from one area to the other. It has been said [27] that the precipitation produced by shallow orographic systems can be underestimated by microwave radiometer algorithms. Also, the presence of dense, cold cirrus clouds often leads to overestimation of rainfall [28]. Therefore, the variability and complexity of the Mexican orography is enough for the IMERG precipitation product to be conditioned by all error sources previously mentioned. On both shores of the country, there are low elevation stations with moist advection coming from the oceans. Inwards of the country, close to the coasts, the presence of high mountainous systems and high plains in the center of the country can be observed in Figure 1b. Therefore, the humidity is forced to rise due to orography, and deep cumulonimbus clouds are formed mainly in summer time, windward of the mountain systems spreading large areas of dense cirrus. This regional situation might easily lead to overestimation of precipitation. Also, one source of precipitation over the high plains in Mexico is from the shallow cumulus clouds that most often form during the dry season. However, during summertime, large convective systems may form during night-time hours leading to the overestimation of precipitation by IMERG.

On the other hand, the analysis of the extreme precipitation events showed a different behavior of the IMERG precipitation estimates. Both hourly and daily cumulative precipitations from IMERG underestimate rain gauge extreme events by more than 60 and 40% of the mean rain gauges respectively. It may seem contradictory that the probability for IMERG to overestimate the hourly precipitation (see Figure 2) increases during night-time hours when there is more probability for precipitation to occur. However, this result is representative of the mean values of the hourly precipitation for which the mode of the precipitation (0 mm) plays an important role. It could also be related with the bilinear interpolation method applied to the IMERG gridded data in order to obtain point values comparable to rain gauges. The extreme events analysis in this study took into consideration the 98th to 99.99th percentiles of the hourly and daily precipitation distributions. The hourly analysis confirms that 98% of the rain gauge data used in this study registered precipitation amounts below 1.2 mm/h and that a large portion of these data may consist of no-precipitation (0 mm/h) cases. Precipitation above the value of 1.2 mm/h are more likely to be underestimated by IMERG. The latter is in agreement with Sharifi et al. [3]. Daily analysis precipitation above 27 mm/day were found to be underestimated by IMERG. However, Figure 8b suggests that this underestimation could still be produced for precipitation intensities below this threshold.

In addition, the daily analysis of precipitation intensities and the elevation shows no relation (Figure 7). IMERG shows no significant deviation when daily precipitations are lower than 10 mm/day; the same as in Ma et al. [4]. However, when precipitations are higher or extreme, deviations of IMERG can be over 15 mm/day per station regardless of its altitude. In Figure 6, it can be noted that IMERG deviates during particular days when precipitation might be considered extreme or intense. *RMSE* values in Figure 2, Tables 2–4 also confirm that the larger the amounts of precipitation, the larger the deviations. Gaona et al. [5] consistently stated that IMERG overestimates rainfall intensities higher than 9 mm/day and attributed it to the fact that extreme rainfall events evolve rapidly, reducing the

probability of the direct detection of such events given the approximate 3-h sampling of the whole GPM satellite constellation.

Furthermore, the accuracy of the IMERG estimates also improves with the time scale. Spatial values of *RBIAS* (Figures 4a and 9a) and *RMSE* (Figures 4b and 9b) are also better for the daily analysis but the trend for IMERG to overestimate mean values is maintained. Also, the *POD* and *CSI* values are closer to 1 for the daily precipitation than for the hourly precipitation. However, the *ACC* is better for the hourly than for the daily precipitation. This happens because *ACC* is sensible to the amount of no-precipitation events which decreases with the time scale. In addition, results found here show that the *FAR* decreases with increasing altitude while the *POD* and the *CSI* increase with increasing altitude (Figures 5 and 9). The mean values of these categorical and the other continuous statistics are consistent with earlier studies [3,4].

Finally, the seasonal analysis showed good results, particularly for the dry season. For the wet season, positive deviations of IMERG may be expected.

5. Conclusions

In this research, the IMERG precipitation data have been evaluated over a Mexican region during the period between 1 April 2014 and 31 October 2015. This assessment has been made for different time scales (hourly, daily and seasonal) using precipitation gauges, as the reference data, from 99 automatic meteorological stations. The main conclusions of the study are summarized below:

The IMERG hourly precipitation product is able to reproduce the diurnal cycle. A small agreement was found with respect to hourly rain gauges with an average *COR* of about 0.35. IMERG tends to overestimate mean hourly values with relatively large deviations. For extreme values of hourly precipitation, its performance is quite poor with a *COR* of 0.18 and a trend to underestimate rain gauges by 61%.

IMERG shows better performance at the daily time scale resolution, with a *COR* of 0.54. An overall bias of 0.34 mm/day over mean daily rain gauges was found. For extreme precipitation events the *COR* (0.36) also improved with respect to the hourly analysis and a trend to underestimate daily rain gauges by 46% was observed. In addition, the deviations of IMERG are minima for precipitation intensities below 10 mm/day and they increase for precipitation rates over this value.

The seasonal analysis showed good results, particularly for the dry season with a *COR* of 0.69 and a positive bias of 1.11 mm. For the wet season a *COR* of 0.51 and positive bias of 96.36 mm was found. For this season, very large deviations of IMERG may be expected.

In terms of categorical statistics, the *FAR*, *POD* and *CSI* values were found to improve from hourly to daily time scales. The *FAR* decreased from 0.7 to 0.4 approximately; the *POD* values increased from 0.5 to 0.8 in average and *CSI* values increased from 0.2 to 0.6. These statistics were also found to improve with topography. However, in this study this relationship becomes more evident for the daily than for the hourly precipitation. While *FAR* values decreased with elevation, *POD* and *CSI* values behaved the other way around.

According to this research, the IMERG hourly precipitation product should be used with caution over Mexico. Users should be aware of its poor performance, especially during heavy rainfall events. The daily and seasonal IMERG precipitation estimates are more reliable. Our findings differ from the suggestions of Tan et al. [6] that IMERG would perform poorer over mountainous areas. This study found that IMERG tends to improve precipitation detection and to decrease magnitude errors over the higher terrain elevations of Mexico. This result could be highly influenced by a non-homogeneous distribution of gauges along the elevation ranges. In order to support our finding, it is advised to include all (daily and synoptic) rain gauges available in the country, which were disregarded in this study due to their relatively low time resolution. However insufficient and sparse these rain gauges are over the region, IMERG is not quite yet an accurate substitute for real observations.

This research is, to our knowledge, the first study to evaluate IMERG precipitation data over Mexico and provides a reference for IMERG users on its performance. Consequently, it opens a window

for future works regarding spatial verification of modeled precipitation and hydrological applications over the region. The results presented in this article are of great value to Mexico where the current precipitation data sources are still insufficient. Also, this study complements previous research and helps in improving our understanding of the IMERG database.

Supplementary Materials: The following are available online at www.mdpi.com/2072-4292/9/5/503/s1, Figure S1: Scatter plot for the 99.99th to 100th percentile of the hourly rain gauges. Rain gauges vs. IMERG from 1 April 2014 to 31 October 2015 over the Mexico region. Table S1: Hourly statistics analysis for 99.99th to 100th percentiles of the hourly precipitation distribution. Other supplementary materials are available upon request. Please contact the main author by email to request this information.

Author Contributions: Yandy G. Mayor realized his Master's thesis project entitled "Hydrometeorological verification of the WRF model on Mexico through satellite observations" in the University Centre for Exact Sciences and Engineering, Guadalajara University, under the supervision of Iryna Tereshchenko. This article is based on research performed subsequent to this earlier project. The initial experiments were realized with the help of Mariam Fonseca Hernández, who also substantially improved this article. Diego A. Pantoja participated in the data collection and contributed to the writing of this paper. Jorge M. Montes Aréchiga gave constructive suggestions about the experiment design and contributed to the writing of this paper.

Conflicts of Interest: The authors declare that there is no conflict of interest regarding the publication of this article.

References

1. Huffman, G.J.; Bolvin, D.T.; Braithwaite, D.; Hsu, K.; Joyce, R.; Kidd, C.; Nelkin, E.J.; Xie, P. *NASA Global Precipitation Measurement (GPM) Integrated Multi-satellitE Retrievals for GPM (IMERG)*; Algorithm Theoretical Basis Doc. Version 4.5; NASA: Greenbelt, MD, USA, 2015; p. 26.

2. Wang, J.; Petersen, W.A.; Wolff, D.B.; Huffman, G.J.; Bolvin, D.T.; Kirstetter, P.E. Validation of Satellite Precipitation Products Using MRMS over the CONUS, Poster Presentation. In Proceedings of the 8th European Conference on Radar in Meteorology and Hydrology, Garmisch-Partenkirchen, Germany, 1–5 September 2014.

3. Sharifi, E.; Steinacker, R.; Saghafian, B. Assessment of GPM-IMERG and Other Precipitation Products against Gauge Data under Different Topographic and Climatic Conditions in Iran: Preliminary Results. *Remote Sens.* **2016**, *8*, 135. [CrossRef]

4. Ma, Y.; Tang, G.; Long, D.; Yong, B.; Zhong, L.; Wan, W.; Hong, Y. Similarity and Error Intercomparison of the GPM and Its Predecessor-TRMM Multisatellite Precipitation Analysis Using the Best Available Hourly Gauge Network over the Tibetan Plateau. *Remote Sens.* **2016**, *8*, 569. [CrossRef]

5. Gaona, M.F.R.; Overeem, A.; Leijnse, H.; Uijlenhoet, R. First-year evaluation of GPM-rainfall over the Netherlands: IMERG day-1 final run (V03D). *J. Hydrometeorol.* **2016**, *17*, 2799–2814. [CrossRef]

6. Tan, J.; Petersen, W.; Kirstetter, P.; Tian, Y. Performance of IMERG as a Function of Spatiotemporal Scale. *J. Hydrometeorol.* **2017**, *18*, 307–319. [CrossRef]

7. Guo, H.; Chen, S.; Bao, A.; Behrangi, A.; Hong, Y.; Ndayisaba, F.; Hu, J.; Stepanian, P.M. Early assessment of integrated multi-satellite retrievals for global precipitation measurements over China. *Atmos. Res.* **2016**, *176–177*, 121–133. [CrossRef]

8. Miranda, J.L.G. Precipitation Estimation over Mexico Applying PERSIANN System and Gauge Data. Master's Thesis, University of Arizona, Tucson, AZ, USA, 2002.

9. García, E. *Modificaciones al Sistema de Clasificación Climática de Köpen*, 5th ed.; CONABIO: México DF, México, 2004.

10. Vera, C.; Higgins, W.; Amador, J.; Ambrizzi, R.; Garreaud, R.; Gochis, D.; Gutzler, D.; Lettenmaier, D.; Marengo, J.; Mechoso, C.R.; et al. Toward a unified view of the American monsoon systems. *J. Clim.* **2006**, *19*, 4977–5000. [CrossRef]

11. Brito-Castillo, L.; Vivoni, E.R.; Gochis, D.; Filonov, A.; Tereshchenko, I.; Monzon, C. An anomaly in the occurrence of the month of maximum precipitation distribution in northwest Mexico. *J. Arid Environ.* **2010**, *74*, 531–539. [CrossRef]

12. Huffman, G.J.; Nelkin, E.J. *Integrated Multi-satellitE Retrievals for GPM (IMERG) Technical Documentation*; NASA Doc.; NASA: Greenbelt, MD, USA, 2015; p. 47.

13. Sims, E.M.; Liu, G. A Parameterization of the Probability of Snow–Rain Transition. *J. Hydrometeorol.* **2015**, *16*, 1466–1477. [CrossRef]

14. Accadia, C.; Mariani, S.; Casaioli, M.; Lavagnini, A.; Speranza, A. Sensitivity of precipitation forecast skill scores to bilinear interpolation and a simple nearest-neighbor average method on high-resolution verification grids. *Weather Forecast.* **2003**, *18*, 918–932. [CrossRef]

15. Lanciani, A.; Mariani, S.; Casaioli, M.; Accadia, C.; Tartaglione, N. A multiscale approach for precipitation verification applied to the FORALPS case studies. *Adv. Geosci.* **2008**, *16*, 3–9. [CrossRef]

16. Ud Din, S.; Al-Dousari, A.; Ramdan, A.; Al Ghadban, A. Site-specific precipitation estimate from TRMM data using bilinear weighted interpolation technique: An example from Kuwait. *J. Arid Environ.* **2008**, *72*, 1320–1328. [CrossRef]

17. Qiao, L.; Hong, Y.; Chen, S.; Zou, C.B.; Gourley, J.J.; Yong, B. Performance assessment of the successive Version 6 and Version 7 TMPA products over the climate-transitional zone in the southern Great Plains, USA. *J. Hydrol.* **2014**, *513*, 446–456. [CrossRef]

18. Liu, Z. Comparison of versions 6 and 7 3-hourly TRMM multi-satellite precipitation analysis (TMPA) research products. *Atmos. Res.* **2015**, *163*, 91–101. [CrossRef]

19. Ebert, E.E.; Janowiak, J.E.; Kidd, C. Comparison of near-real-time precipitation estimates from satellite observations and numerical models. *Bull. Am. Meteorol. Soc.* **2007**, *88*, 47–64. [CrossRef]

20. Bharti, V.; Singh, C. Evaluation of error in TRMM 3B42V7 precipitation estimates over the Himalayan region. *J. Geophys. Res. Atmos.* **2015**, *120*, 12458–12473. [CrossRef]

21. Wilks, D. *Statistical Methods in the Atmospheric Sciences*, 2nd ed.; Academic Press: San Diego, CA, USA, 2006; p. 627.

22. Tan, J.; Petersen, W.; Tokay, A. A Novel Approach to Identify Sources of Errors in IMERG for GPM Ground Validation. *J. Hydrometeorol.* **2016**, *17*, 2477–2491. [CrossRef]

23. Cleveland, W.S. Robust locally weighted regression and smoothing scatterplots. *J. Amer. Stat. Assoc.* **1979**, *74*, 829–836. [CrossRef]

24. Tang, G.; Ma, Y.; Long, D.; Zhong, L.; Hong, Y. Evaluation of GPM Day-1 IMERG and TMPA version-7 legacy products over mainland China at multiple spatiotemporal scales. *J. Hydrol.* **2016**, *533*, 152–167. [CrossRef]

25. Kikuchi, K.; Wang, B. Diurnal precipitation regimes in the global tropics. *J. Clim.* **2008**, *21*, 2680–2696. [CrossRef]

26. Chen, F.; Li, X. Evaluation of IMERG and TRMM 3B43 monthly precipitation products over mainland China. *Remote Sens.* **2016**, *8*, 472. [CrossRef]

27. Shige, S.; Kida, S.; Ashiwake, H.; Kubota, T.; Aonashi, K. Improvement of TMI rain retrievals in mountainous areas. *J. Appl. Meteorol. Climatol.* **2013**, *52*, 242–254. [CrossRef]

28. Liou, K.N. *Cirrus Clouds and Climate, Yearbook of Science & Technology*, 1st ed.; McGraw Hill: Columbus, OH, USA, 2005; pp. 51–53.